# Computationally determined existence and stability of transverse structures. I. Periodic optical patterns

G. K. Harkness, W. J. Firth,* G.-L. Oppo,† and J. M. McSloy‡
*Department of Physics, University of Strathclyde, 107 Rottenrow, Glasgow G4 ONG, Scotland*
(Received 31 May 2002; published 10 October 2002)

We present a Fourier-transform based, computer-assisted, technique to find the stationary solutions of a model describing a saturable absorber in a driven optical cavity. We illustrate the method by finding essentially exact hexagonal and roll solutions as a function of wave number and of the input pump. The method, which is widely applicable, also allows the determination of the domain of stability (Busse balloon) of the pattern, and sheds light on the mechanisms responsible for any instability. To show the usefulness of our numerical technique, we describe cracking and shrinking patches of patterns in a particular region of parameter space.

DOI: 10.1103/PhysRevE.66.046605 PACS number(s): 42.65.Tg, 42.50.Md, 42.65.Sf

## I. INTRODUCTION

Over the last few years, a large variety of optical systems have been shown theoretically, and demonstrated experimentally, to produce self-organized structures in the cross section of their output beams. Among such systems are saturable absorbers or Kerr media in cavities, gas cells, liquid-crystal light values, and semiconductor microresonators [1–6]. Because of the speed and possible compactness of optical devices, such phenomena have the potential for applications in information storage and processing [7,8].

The structures observed fall mainly into two classes: localized structures (e.g., cavity solitons [3]) and extended, periodic patterns. It is the latter on which we focus in this paper because techniques similar to those we discuss here have already been applied to the former in our companion paper [9] and [10–12].

We have developed a computer-assisted technique (Sec. III), valid for arbitrary values of the system parameters, which can find the stationary solutions of nonlinear partial differential equations such as those used to model the above systems. It uses a Newton-type method and a Fourier transform to evaluate the spatial derivatives. The Newton method automatically gives the linearization around the found solutions and therefore the method is easily extended to find their eigenspectrum and the spatial form of any eigenmode. Thus, the stability of the pattern can be determined, as can the nature of any instability.

In Secs. IV and V, this method will be demonstrated by finding abitrarily accurate roll and hexagonal solutions for a model of a saturable absorber in a driven optical cavity. These patterned solutions will be shown as a function of their wave number and intensity of the homogeneous solution with which they coexist, the latter being a convenient parametrization of the input driving field. We hence find the patterns' domain of stability—known as the *Busse balloon* [13]. In optics, this domain has previously only, to the best of our knowledge, been calculated for traveling waves and amplitude equation patterns in lasers [14–16], where the problem is much simpler because these patterns are known explicitly in analytic form. We confirm our stability analysis by numerically simulating the dynamical evolution of typical roll and hexagonal patterns, and present some interesting scenarios in which we accurately determine where these patterns lose stability and the mechanisms by which they do so. Finally, Sec. VI provides a brief conclusion.

## II. MODEL

We demonstrate our approach using the example of a saturable absorber in a cavity, first introduced in this context in [1], and subsequently studied in some detail in [7,9,17–21]. Although we have chosen a particular model system, our technique should be very widely applicable for pattern-forming models, whether in optics or other fields of science. We also expect that qualitatively similar instability scenarios can be found adjacent to the Busse balloon of many other systems.

Our system is usually described using the following partial differential equation [1,7]:

$$\partial_t E = -E\left((1+i\theta)+\frac{2C}{1+|E|^2}\right)+E_I+i\nabla_\perp^2 E, \qquad (1)$$

where $E(x,y,t)$ is the slowly varying amplitude of the intracavity electric field. The time $t$ is scaled to a cavity lifetime $\tau$ and $\nabla_\perp^2$ is the transverse Laplacian $\partial_x^2+\partial_y^2$. The cavity contains an ensemble of two-level atoms and is driven by a plane-wave input field $E_I$, assumed to be resonant in frequency with the atomic transition. The field is detuned by $\theta$ from the nearest longitudinal cavity mode. The ‘‘cooperativity'' parameter $C$ gives the aggregate strength of the coupling between the cavity field and the atoms.

We choose $\theta=-1.2$ in which case this equation has a unique stationary, spatially homogeneous solution $E=E_0$. The corresponding intracavity intensity $I=|E_0|^2$ is thus also unique, and is a more convenient control parameter than $E_I$ itself. We also define a field $A$ through $E=E_0(1+A)$, which obeys the following equation, fully equivalent to Eq. (1):

*Electronic address: willie@phys.strath.ac.uk
†Electronic address: gianluca@phys.strath.ac.uk
‡Electronic address: jmc@phys.strath.ac.uk

 

$$\partial_t A = -(1+i\theta)A + \frac{2C}{1+I} - \frac{2C(1+A)}{1+I(1+A)(1+A^*)} + i\nabla_\perp^2 A. \qquad (2)$$

Linear stability analysis of the trivial homogeneous solution $A=0$ of Eq. (2) (or of $E=E_0$ of Eq. (1) [1]) shows that it is stable outside the range $I_c<I<I_u$ where $I_{c,u}$ are the roots of $(I+1)^2=2C(I-1)$. We take $C=5.4$, giving $I_c=1.65$. Perturbations with spatial wave-vector $k_c=\sqrt{-\theta}$ have positive growth rate across the entire unstable range, leading to hexagonal or roll patterns, depending on parameter values [17]. No nontrivial analytic solutions of Eq. (2) are known, however, and so the nature and stability of these patterns have to be determined numerically. This can be done with straightforward simulation of the partial differential equation [17], but this approach is limited in practice to stable solutions, and typically requires long integration times for parameter scans, especially in two dimensions (2D). In the next section, we adopt a different approach, in which we use computer techniques to find essentially exact stationary solutions to Eq. (2), and determine their stability.

## III. NUMERICAL TECHNIQUES

We aim first to determine nontrivial stationary field distributions $A=A_s(\mathbf{r})$ for Eq. (2). We do this by setting the left-hand side equal to zero and solving the resulting boundary-value problem. In other works, this approach has been used to study localized solutions to this and related equations [2,7,9,11,12], but here we look for periodic patterns, either stripes (rolls) or hexagons. Rolls and hexagons, and also square and honeycomb solutions have been found using a different approach, in which the desired pattern is selected, and if necessary stabilized, by Fourier filtering [20], but that method was not used to systematically study the stability of patterns, e.g., as a function of wavevector.

To allow us flexibility in studying different types of periodic solutions, we define a set of basis vectors $\mathbf{T}_1$ and $\mathbf{T}_2$ such that they are the smallest vectors which satisfy

$$A_s(\mathbf{r}) = A_s(\mathbf{r}+n\mathbf{T}_1+m\mathbf{T}_2),$$

$n$ and $m$ being integers. For example, vectors of equal length, separated by $\pi/3$ give a unit cell for hexagons with spatial wave-vector $k=2\pi/|\mathbf{T}_1|$. Such periodic solutions can therefore be represented by their "unit cell" $A_s(\mathbf{r})=A_s(r_1\mathbf{T}_1+r_2\mathbf{T}_2)$ where $r_1$ and $r_2$ lie in the range (0,1).

Numerically, we will represent this unit cell $A_s(\mathbf{r})$ on a regular grid of typically $16\times16$ $(r_1,r_2)$ values. We can compute the Laplacian term in Eq. (2) by using a fast Fourier transform. The real-space basis vectors $\mathbf{T}_1$ and $\mathbf{T}_2$ define an associated Fourier space with basis vectors $\mathbf{K}_1$ and $\mathbf{K}_2$ such that $\mathbf{T}_i.\mathbf{K}_j=\delta_{ij}$. The Laplacian is computed by taking a Fourier transform, multiplying by $-|\mathbf{K}|^2=-|(k_1\mathbf{K}_1+k_2\mathbf{K}_2)|^2$, and taking an inverse Fourier transform.

An initial guess at a stationary solution $A_s(r_1,r_2)$ can be refined iteratively using a Newton method to converge to an accurate stationary solution to Eq. (2). This process can be repeated for a range of values of the control parameter $I$ and the magnitude of the pattern's spatial wave-vector $k$. Note that patterns typically exist over a *continuum* of $k$, and that even though we discretize the field within the unit cell, we can set $k$'s value to machine precision. This enables us to meaningfully distinguish between patterns with arbitrarily close values of $k$, and so we can accurately determine the boundary of the Busse Balloon. In contrast, a simulation method can only find solutions periodic on the simulation grid, so to determine anything other than a very coarse $k$ dependence of, e.g., stability is prohibitive in terms of computer resource.

Simulation techniques have a similar difficulty with the perturbation stability of a pattern. Since one can only test stability with regard to grid-compatible perturbations, one can only get a coarse representation of the spatial instability spectrum. In contrast, our method is easily adapted to find the stability of a given pattern to perturbations of *any* wave vector, whether commensurate or not.

We make the ansatz

$$A(\mathbf{r}) = A_s(\mathbf{r}) + u_{\mathbf{dk}}(\mathbf{r})\exp(i\,\mathbf{dk}\cdot\mathbf{r}) + v^*_{\mathbf{dk}}(\mathbf{r})\exp(-i\,\mathbf{dk}\cdot\mathbf{r}).$$

By analogy with Bloch functions in solid-state physics, $u_{\mathbf{dk}}(\mathbf{r})$ and $v_{\mathbf{dk}}(\mathbf{r})$ have the same periodicity as $A_s(\mathbf{r})$ and $\mathbf{dk}$ can be *any* vector within the "Brillouin zone," meaning that $\mathbf{dk}=dk_1\mathbf{K}_1+dk_2\mathbf{K}_2$ with $-\pi/|\mathbf{T}_i|<dk_i<\pi/|\mathbf{T}_i|$.

Inserting this ansatz into the discretized Eq. (2) and linearizing in $u$ and $v$ gives a matrix problem as a function of $\mathbf{dk}$,

$$\frac{d}{dt}\begin{pmatrix} u \\ v \end{pmatrix} = J\begin{pmatrix} u \\ v \end{pmatrix},$$

where $J$ is a matrix. For a grid of $16\times16$ $(r_1,r_2)$ values, $J$ is typically of size $512\times512$. The resulting eigenproblem is easily solved on modern workstations, leading to eigenvalues $\lambda(\mathbf{dk})$. By performing this analysis for appropriate values or ranges of $\mathbf{dk}$, the stability of the pattern can be determined. Of course the computer time needed to explore the entire Brillouin zone may be substantial, but there is no intrinsic or memory-related limit to the completeness of this stability analysis.

If any eigenvalue, for any $\mathbf{dk}$ within the Brillouin zone, has a positive real part, then the solution found is unstable. There exist two neutral modes, $\lambda=0$, for $\mathbf{dk}=0$, corresponding to the two-dimensional translational symmetry of Eq. (2). Thus, any pattern is at best neutrally stable, but we will concentrate on stability against modes other than these neutral modes, and if all such modes have eigenvalues with negative real parts we will regard the pattern as stable.

In this way, stationary patterned solutions to Eq. (2) can be found as a function of two continuous variables: the control parameter $I$ and the pattern's wave vector $k$. Further-more, the linear stability of any pattern can be assessed by evaluating the growth rate of perturbations with an arbitrary wave vector.

### IV. ROLL EXISTENCE AND STABILITY

To show the effectiveness of this technique, let us demonstrate this procedure for stripes (rolls). In this case, $A_s(x)$, and so $\mathbf{T}_1=2\pi\hat{\mathbf{x}}/k$, $\mathbf{T}_2=0\hat{\mathbf{y}}$. This raises a technical point, in that $\mathbf{K}_2$ should be infinite. This is however not a problem in practice. Both the computation of the solution and its 2D stability can be found by a one-dimensional calculation, where $dk_2$ enters the computation only as a parameter. In principle, $dk_2$ has an infinite range, but in practice it need only be explored over a range similar to that used for $dk_1$—see Fig. 3.

Figure 1 tracks the roll solution with $k=k_c$. The roll amplitude is represented by the integral $\int|A|dxdy$, which is a convenient, if unphysical, representation of the modulation depth of these patterns. The homogeneous solution $A=0$ (solid line) becomes unstable to perturbations with $k=k_c$ at the value of $I=I_{\mathrm{mi}}(k_c)$ where the suffix $mi$ stands for modulational instability. The roll solution (dashed line) bifurcates subcritically at this point, forming a solution branch leading to a saddle-node point at $I=I_{\mathrm{sn}}(k_c)$. Here the solution curve turns to form an "upper"-solution branch, which eventually terminates at $I=I_u=7.15$. The dotted line marked $I_{lk}$ in Fig. 1 is the locking limit of localized stripe solutions, the behavior of which is described and analyzed in the companion paper [9] and [23].

Our solution method can find solutions with any value of $k$, and test their stability. Figure 2 maps the existence and stability of rolls in a portion of the $(k/k_c, I)$ plane. The traversing lines marked by $I_{\mathrm{sn}}(k)$ and $I_{\mathrm{mi}}(k)$ are the limit of pattern existence and of modulational instability of the homogeneous solution, respectively. They cut the line $k=k_c$ at $I=I_{\mathrm{sn}}$ and $I=I_{\mathrm{mi}}$ designated on Fig. 1, which can thus be viewed as a section of a surface of which Fig. 2 is a top view.

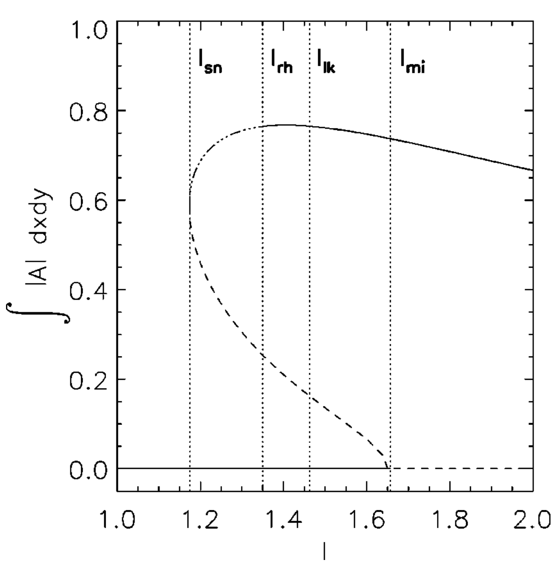


FIG. 1. Existence behavior of rolls with wave vector $k_c$ and plotted as a function of $I$. Solutions are stable on the solid and unstable on the dashed lines. The dash-dotted line indicates where the roll pattern is unstable to the formation of hexagons. Parameters are $C=5.4$ and $\theta=-1.2$.

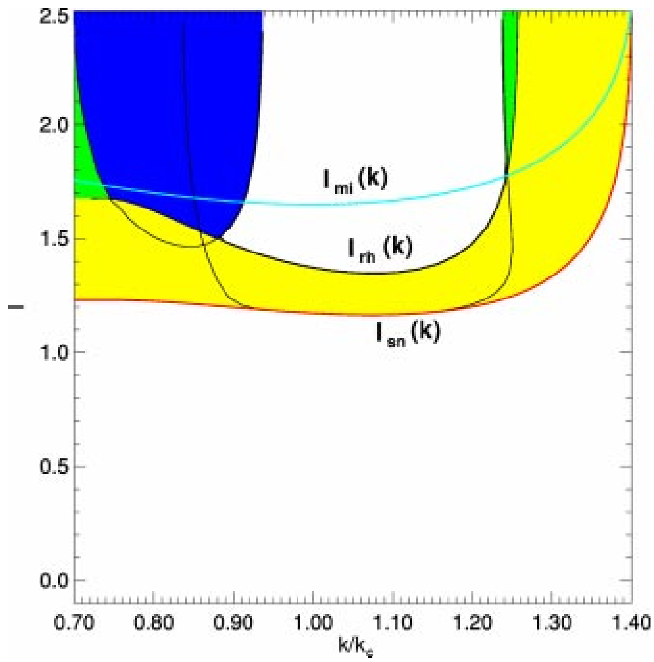


FIG. 2. Existence regimes of roll patterns plotted as a function of $k/k_c$ and $I$. The traversing lines marked by $I_{\mathrm{sn}}(k)$ and $I_{\mathrm{mi}}(k)$, respectively, are the limit of pattern existence and modulational instability of the homogeneous solution. Enclosed white, light gray, dark gray, and black areas, respectively, denote regions where roll solutions are stable, unstable to hexagons, Eckhaus unstable, and zigzag unstable. Parameters are $C=5.4$ and $\theta=-1.2$.

From Figs. 1 and 2 it can be seen that between $I=I_{\mathrm{sn}}(k)$ and $I=I_{\mathrm{mi}}(k)$ the roll solutions coexist with a stable homogeneous solution. This is the region where, as expected, we can find localized stripe solutions to Eq. (2) [7].

The shaded areas, and their associated boundaries in Fig. 2, show roll instabilities of different characters, which we determine by analyzing the perturbation stability of a given roll (represented by a point in Fig. 2) over its Brillouin zone.

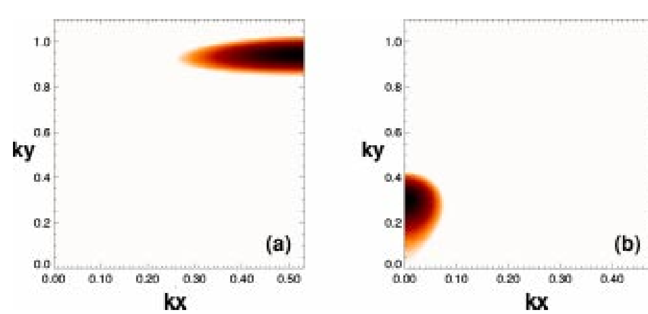


FIG. 3. Left and right panels, respectively, show the roll to hexagon amplitude instability and maximum growth of zigzag instability with **dk** perpendicular to **k**. In the dark areas, perturbations have a postive growth rate, and thus the pattern is unstable. Parameters are (a) $k=k_c$, $I=1.37$; (b) $k/k_c=0.88$, $I=2.1$; other parameters $C=5.4$ and $\theta=-1.2$.

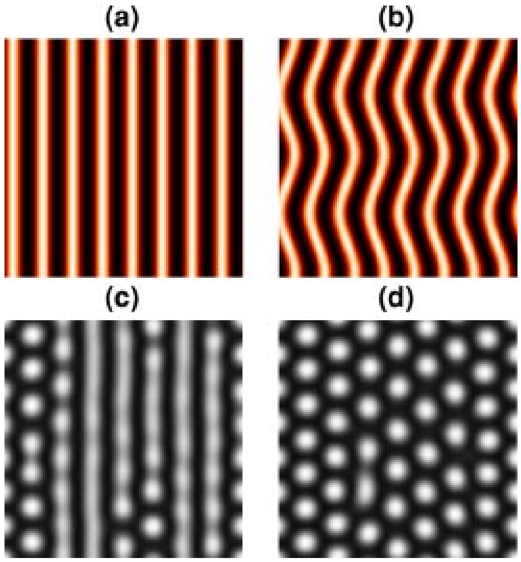


FIG. 4. Roll patterns from stability regions in Fig. 2. (a) Stable roll pattern from Busse balloon with $I=1.6$ and $k/k_c=1.10$. (b) Zigzag unstable roll pattern, $I=2.1$ and $k/k_c=0.88$). Panels (c) and (d) show the evolution of the amplitude instability associated with rolls when $k=k_c$ at $I=1.37$, respectively, $\tau=150$ and 300. Parameters are $C=5.4$, $\theta=-1.2$, and $\tau$ is the time scaled to a cavity lifetime.

Figure 3 illustrates these calculations. On the left, $k$ and $I$ lie in the domain of zigzag instability, and there are growing modes around $k_y/k_c=0.3$, indicating a transverse instability of the stripes. This results in a periodic lateral deformation. On the right, the roll is unstable to hexagon formation, and the most unstable perturbation vector is oblique. The corresponding eigenmode induces a longitudinal modulation of each stripe, creating chains of spots, but with a phase shift between the spot locations on neighboring stripes. This corresponds to the formation of hexagons rather than, say, squares.

In the dark gray area, the rolls are Eckhaus unstable, which is an instability with **dk** parallel to **k** [22]. This leads to a shift in the wave vector of the pattern, pulling it closer to a "preferred" value of $k$ within the white area above $I=I_{\mathrm{rh}}$.

This domain is known as the Busse balloon [13], where the rolls are absolutely stable against all small perturbations. For example, looking at the part of the Busse balloon below the modulational instability threshold, we observe that a roll pattern with any wave vector between about $0.91k_c$ and $1.23k_c$ is stable against *all* perturbations. Since $k_c$ in our case corresponds to the wave vector with the highest growth rate, simulations starting from the now unstable homogeneous state relax to a $k_c$ patterned state. Simulations started with the wave vector within the Busse balloon, however, remain fixed at their initial value of $k$. The accurate determination of the Busse balloon is one of the key results of this paper and a major strength of our computer-assisted approach to pattern existence and stability. Note that this method reveals symmetry-breaking, as well symmetry-preserving instabilities.

The predicted instabilities are fully confirmed by numerical simulation, as illustrated in Fig. 4, in which panel (a) demonstrates the stability of a roll inside the Busse balloon,

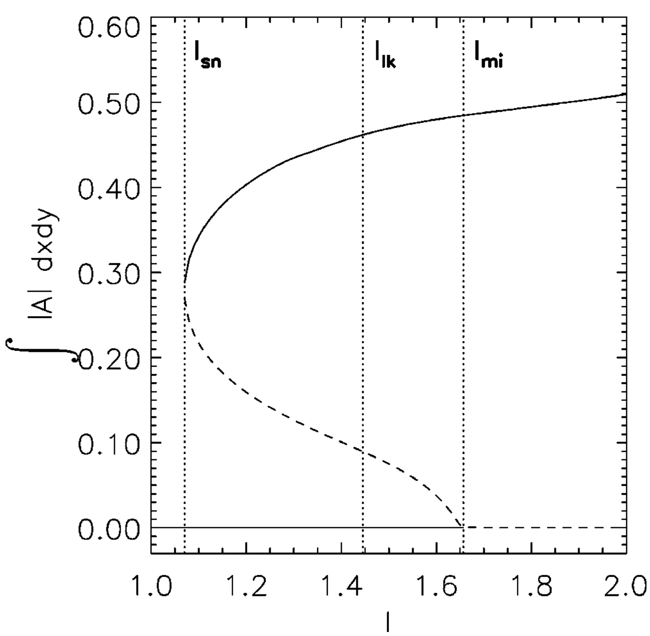


FIG. 5. Existence behavior of hexagons with wave vector $k_c$ and plotted as a function of $I$. Solutions are stable on the solid and unstable on the dashed lines. Parameters are $C=5.4$ and $\theta=-1.2$.

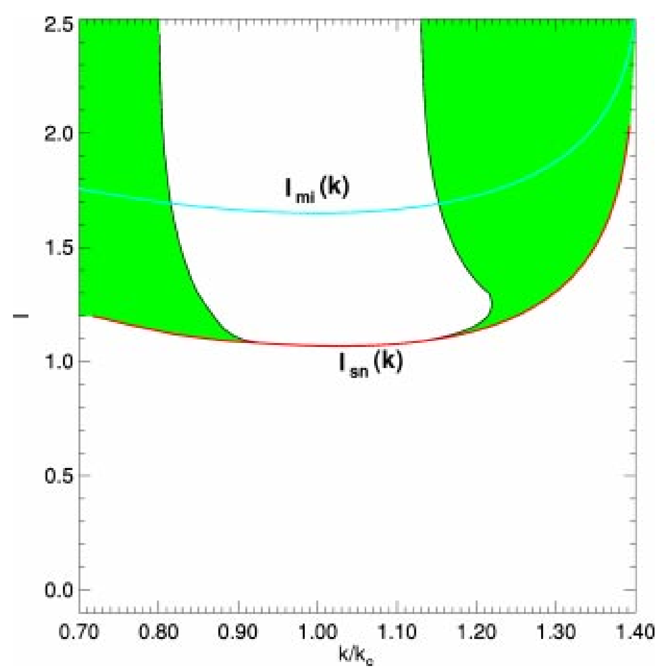


FIG. 6. Existence regimes of hexagonal patterns plotted as a function of $k/k_c$ and $I$. Enclosed white and gray areas, respectively, correspond to regions where hexagon solutions are stable and Eckhaus unstable. The lowest black and light traversing lines are again labled $I_{\mathrm{sn}}(k)$ and $I_{\mathrm{mi}}(k)$, and, respectively, are the limit of pattern existence and modulational instability of the homogeneous solution. Parameters are $C=5.4$ and $\theta=-1.2$.

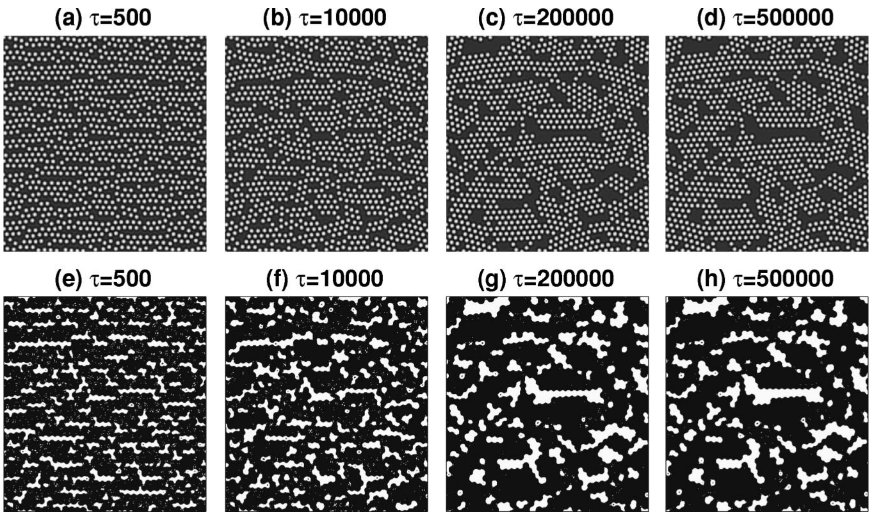


FIG. 7. Dynamical evolution of Eckhaus unstable "cracking" hexagonal pattern of initial wave vector $0.78k_c$. Respectively, shown on top and bottom rows are $|A|$ and negative images showing homogeneous islands (white) and hexagonal seas (black) of $|A|$. Parameters are $I=1.25$, $C=5.4$, and $\theta=-1.2$.

while panels (b)–(d) correspond to the conditions given in Fig. 3.

## V. HEXAGON EXISTENCE AND STABILITY

To further indicate the power of our numerical technique, Figs. 5 and 6 show the bifurcation behavior and stability diagram for a hexagonal solution. Again, the solution bifurcates subcritically from $I=I_{\mathrm{mi}}(k)$ and leads to a saddle-node point at $I=I_{\mathrm{sn}}(k)$. The gray shaded regions are of an Eckhaus-type instability. The line marked $I_{\mathrm{lk}}$ in Fig. 5 is the locking limit of hexagonal clusters of cavity solitons as analyzed in [9].

The shaded area of Fig. 6 corresponding to $k/k_c<1$ is comprised of two distinct regions. Of particular interest here is the Eckhaus unstable area with $k<k_c$ below $I_{\mathrm{mi}}$ where the homogeneous solution is still stable. In this region, the spacing between the spots of the hexagons is too large and the system "prefers" to pack them closer together. The instability leads to local contraction of patches of the hexagonal pattern. The contraction mechanism results in "cracks" appearing between these patches, filled initially, with the homogeneous solution $A=0$. If $I>I_{\mathrm{lk}}$, these cracks are filled by the nucleation of new spots. Dynamically this process looks like "raindrops" falling into the pattern. In this case, if we denote the initial wave vector by $k$, and that of the left edge of the Busse balloon by $k_{\mathrm{bl}}(I)$, the total number of spots increases by a factor $(k_{\mathrm{bl}}/k)^2$, until it reaches the "population" of spots of a stable hexagonal pattern. Since this new solution lies within the Busse balloon, it is stable and no more dynamics are observed.

Figures 7(a)–7(d) show the dynamical evolution of a "cracking" pattern for $I<I_{\mathrm{lk}}$, where the homogeneous solution $A=0$ is stable. The "sea" of hexagons contracts and "islands" of homogeneity are generated. Panels (e)–(h) of Fig. 7 display the same dynamics where regions occupied by hexagons are colored in black and homogeneous regions in white. Such dynamics are observed in a transverse domain of $32\times 2\pi/k_0$ diffraction lengths, and computed on a computational mesh of $512\times 512$ gridpoints, where $k_0=0.78k_c$ is the initial wave vector. It should also be noted that the only noise present in the simulation is that intrinsically contained within the numerics. It can be seen that due to the homogeneous solution $A=0$ being stable, the cracks persist and lead to a series of localized "islands" of homogeneity in an hexagonal "sea." A very slow dynamics of coalescence of homogeneous islands take place. The growth law associated to such a slow process (if any) and a statistical characterization of the cracking patterns will be given elsewhere. Here, we present in Fig. 8 the evolution in Fourier space of the cracking process by using its spectral density. We find that the most prominent wave vector during the later stages of the simulation is approximately $0.92k_c$. This suggests that such hexagonal "islands" are localized hexagonal patterns of the

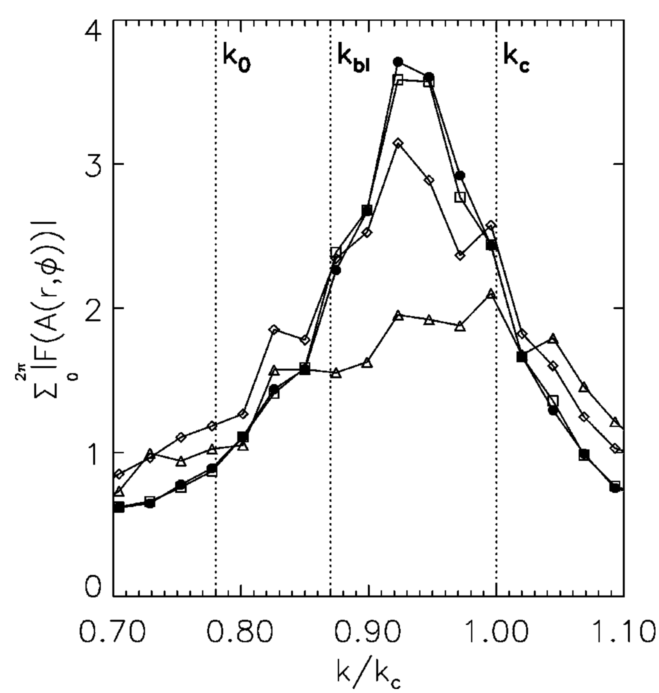


FIG. 8. Spectral density plotted as functions of $k/k_c$. Triangles, diamonds, squares, and dots, respectively, correspond to cracking at $\tau=500$, 10 000, 200 000, and 500 000 as shown in Fig. 7. $F(A)$ is the Fourier transform of the background free field $A$. Parameters are $I=1.25$, $C=5.4$, and $\theta=-1.2$.

Busse balloon where $k_n$ lies approximately half way between $k_c$ and $k_{\mathrm{bl}}(I)$. By purely geometrical arguments, the relative areas $A_{\mathrm{sea}}/A_{\mathrm{land}}=1-(k/k_n)^2$, where $k_n$ is the wave vector characterizing the now-relaxed hexagonal "sea." It should be noted though, that at the boundaries and in the vicinity of defects of the hexagonal regions, the separation of peaks obeys the same law as that presented for clusters of cavity solitons in [21], where $k_n \approx k_{\mathrm{bl}}(I)$. This effect has an analogy in solid-state crystals, where the spacing between atoms at the surface is greater than those in the bulk of the medium.

Finally, for $k>k_c$, the Eckhaus instability leads to the coalescing of spots (Fig. 9, panel b). In some cases, this produces local structures which look like rolls, which may or may not be stable. When they are stable, the resulting pattern looks like hexagons interspersed with localized stripes.

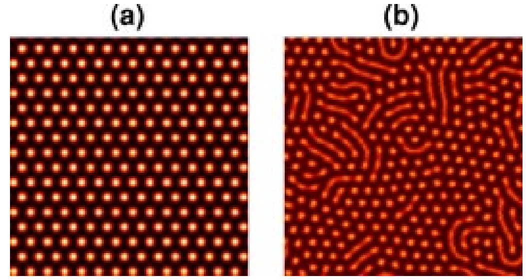


FIG. 9. Hexagonal patterns from stabiliy regions in Fig. 6. Left: stable hexagonal pattern from Busse balloon at $I=1.4$ and wave vector of $k_c$. Right: Eckhaus unstable hexagonal pattern with $I=2.15$ and wave vector of $1.8k_c$. Parameters are $C=5.4$ and $\theta=-1.2$.

## VI. CONCLUSIONS

We have demonstrated a powerful numerically based technique for the calculation of existence and stability of patterns in a staturable absorber optical system. Roll and hexagon solutions with their respective stability regimes were identified including their Busse balloons. Symmetry-breaking and preserving instabilities were identified and mechanisms responsible were determined. Our numerical technique is also useful to identify regions of parameter space where novel spatial structures develop. For example the cracking hexagons of Sec. V have not been described before to the best of our knowledge, and have relevance in the spatiotemporal dynamics of a wide class of systems in optics and also in other fields of science.

## ACKNOWLEDGMENTS

We would like to thank A.J. Scroggie for important discussions relating to this paper. The authors acknowledge financial support from EPSRC Grant Nos. GR/M 31880 and GR/M 19727, SHEFCA/GS0079 Project VISION [24], ESPRIT LTR Project No. 28235 (PIANOS) [8], and QUANTIM (IST-2000-26019). G.-L.O. acknowledges support from SGI.

[1] L.A. Lugiato and C. Oldano, Phys. Rev. A **37**, 3896 (1988).
[2] L.A. Lugiato and R. Lefever, Phys. Rev. Lett. **58**, 2209 (1987).
[3] W.J. Firth and C.O. Weiss, Opt. Photonics News **13**, 54 (2002).
[4] B. Schäpers, M. Feldmann, T. Ackemann, and W. Lange, Phys. Rev. Lett. **85**, 748 (2000).
[5] G.K. Harkness, G.-L. Oppo, E. Benkler, M. Kreuzer, R. Neubecker, and T. Tschudi, J. Opt. B: Quantum Semiclassical Opt. **1**, 177 (1999).
[6] A. Schreiber, B. Thüring, M. Kreuzer, and T. Tshudi, Opt. Commun. **136**, 415 (1997).
[7] W.J. Firth and A.J. Scroggie, Phys. Rev. Lett. **76**, 1623 (1996).
[8] Processing of Information by Arrays of Non-linear Optical Solitons homepage: www.pianos-int.org
[9] J. M. McSloy, G. K. Harkness, G.-L. Oppo, and W. J. Firth, Phys. Rev. E **66** , 046606 (2002).
[10] W.J. Firth and G.K. Harkness, Asian J. Phys. **7**, 665 (1998).
[11] T. Maggipinto, M. Brambilla, G.K. Harkness, and W.J. Firth, Phys. Rev. E **62**, 8726 (2000).
[12] G.-L. Oppo, A.J. Scroggie, and W.J. Firth, Phys. Rev. E **63**, 066209 (2001).
[13] R.M. Clever and F.H. Busse, J. Fluid Mech. **65**, 625 (1974).
[14] G.K. Harkness, W.J. Firth, J.B. Geddes, J.V. Moloney, and E.M. Wright, Phys. Rev. A **50**, 4310 (1994).
[15] P.K. Jakobsen, J. Lega, Q. Feng, M. Staley, J.V. Moloney, and A.C. Newell, Phys. Rev. A **49**, 4189 (1994).
[16] J. Lega, P.K. Jakobsen, J.V. Moloney, and A.C. Newell, Phys. Rev. A **49**, 4201 (1994).
[17] W.J. Firth and A.J. Scroggie, Europhys. Lett. **26**, 521 (1994).
[18] A. J. Scroggie, Ph.D. thesis, University of Strathclyde, Glasgow, 1995.
[19] W.J. Firth, A. Lord, and A.J. Scroggie, Phys. Scr. T **67**, 12 (1996).
[20] R. Martin, A.J. Scroggie, G.-L. Oppo, and W.J. Firth, Phys. Rev. Lett. **77**, 4007 (1996).
[21] A.G. Vladimirov, J.M. McSloy, D.V. Skryabin, and W.J. Firth, Phys. Rev. E **65**, 046606 (2002).
[22] W. Eckhaus, *Studies in Non-Linear Stability Theory* (Springer-Verlag, Berlin, 1965).
[23] Y. Pomeau, Physica D **23**, 3 (1986).
[24] VISION project homepage: www.vision.strath.ac.uk